

Evaluating Signs of Microangiopathy Secondary to Diabetes in Different Areas of the Retina with Swept Source OCTA

Sonja G. Karst,^{1,2} Morgan Heisler,³ Julian Lo,³ Nathan Schuck,¹ Abdollah Safari,⁴ Marinko V. Sarunic,³ David A. L. Maberley,¹ and Eduardo V. Navajas¹

¹Department of Ophthalmology & Visual Sciences, University of British Columbia, Vancouver, British Columbia, Canada

²Department of Ophthalmology and Optometry, Medical University Vienna, Vienna, Austria

³School of Engineering Science, Simon Fraser University, Burnaby, British Columbia, Canada

⁴Faculty of Pharmaceutical Sciences, University of British Columbia, Vancouver, British Columbia, Canada

Correspondence: Eduardo V. Navajas, Department of Ophthalmology & Visual Sciences, Faculty of Medicine, Eye Care Centre (VGH), 2550 Willow Street, Vancouver V5Z 3N9, BC Canada; edunavajas@gmail.com.

Received: September 17, 2019

Accepted: March 24, 2020

Published: May 11, 2020

Citation: Karst SG, Heisler M, Lo J, et al. Evaluating signs of microangiopathy secondary to diabetes in different areas of the retina with swept source OCTA. *Invest Ophthalmol Vis Sci.* 2020;61(5):8. <https://doi.org/10.1167/iovs.61.5.8>

PURPOSE. The purpose of this study was to compare perfusion parameters of the parafovea with scans outside the parafovea to find an area most *susceptible* to changes secondary to diabetic retinopathy (DR).

METHODS. Patients with different DR severity levels as well as controls were included in this cross-sectional clinical trial. Seven standardized 3 × 3 mm areas were recorded with Swept Source Optical Coherence Tomography Angiography: one centered on the fovea, three were temporal to the fovea, and three nasally to the optic disc. The capillary perfusion density (PD) of the superficial capillary complex (SCC) and deep capillary complex (DCC) as well as the fractal dimension (FD) were generated. Statistical analyses were done with R software.

RESULTS. One hundred ninety-two eyes (33 controls, 51 no-DR, 41 mild DR, 37 moderate/severe DR, and 30 proliferative DR), of which 105 patients with diabetes and 25 healthy controls were included (59 ± 15 years; 62 women). Mean PD of the DCC was significantly less in patients without DR (parafovea = 0.48 ± 0.03; temporal = 0.48 ± 0.02; and nasal = 0.48 ± 0.03) compared to controls (parafovea = 0.49 ± 0.02; temporal = 0.50 ± 0.02; and nasal = 0.50 ± 0.03). With increasing DR severity, PD and FD of the SCC and DCC further decreased.

CONCLUSIONS. Capillary perfusion of the retina is affected early by diabetes. PD of the DCC was significantly reduced in patients with diabetes who did not have any clinical signs of DR. The capillary network outside the parafovea was more susceptible to capillary perfusion deficits compared to the capillaries close to the fovea.

TRIAL REGISTRATION. clinicaltrials.gov, NCT03765112, <https://clinicaltrials.gov/ct2/show/NCT03765112?term=NCT03765112&rank=1>

Keywords: diabetic retinopathy, OCT angiography, retinal blood flow

Diabetic retinopathy (DR) affects about one third of patients with diabetes, estimated at 145 million people worldwide.¹ DR severity grading is typically based on the evaluation of retinal lesions visible in fundus biomicroscopy or fundus photography. As DR severity increases, so does the risk of vision-threatening complications. Microvascular changes preceding DR include endothelial cell loss followed by scattered nonperfusion of retinal capillaries, which is commonly not readily accessible in the standard clinical examination.

Optical coherence tomography angiography (OCTA) is a fairly new technology to image the vascular networks of the retina in a fast and noninvasive way. The retinal capillary networks can be resolved separately and capillary dropout can be quantified accordingly. In DR, capillary perfusion density (PD) and capillary branching complexity (fractal

dimension [FD]) are known to decrease with advanced DR severity.^{2–9} First, differences in perfusion parameter between nonproliferative diabetic retinopathy (NPDR) and healthy controls were described mainly in the superficial capillary plexus, whereas other groups emphasized the importance of the deep capillary complex (DCC) in the pathogenesis of DR.^{10–15}

Capillary perfusion parameters in patients with diabetes were predominately analyzed in the parafovea and the peripapillary region,^{5,11,16} whereas DR affects the entire retina and not primarily the fovea.^{17,18} It is still unknown to which extent the capillary bed outside the parafovea is affected by diabetes.

The parafoveal circulation differs from the rest of the retina. In the parafovea, three capillary networks of the retina can be distinguished while the intermediate and deep

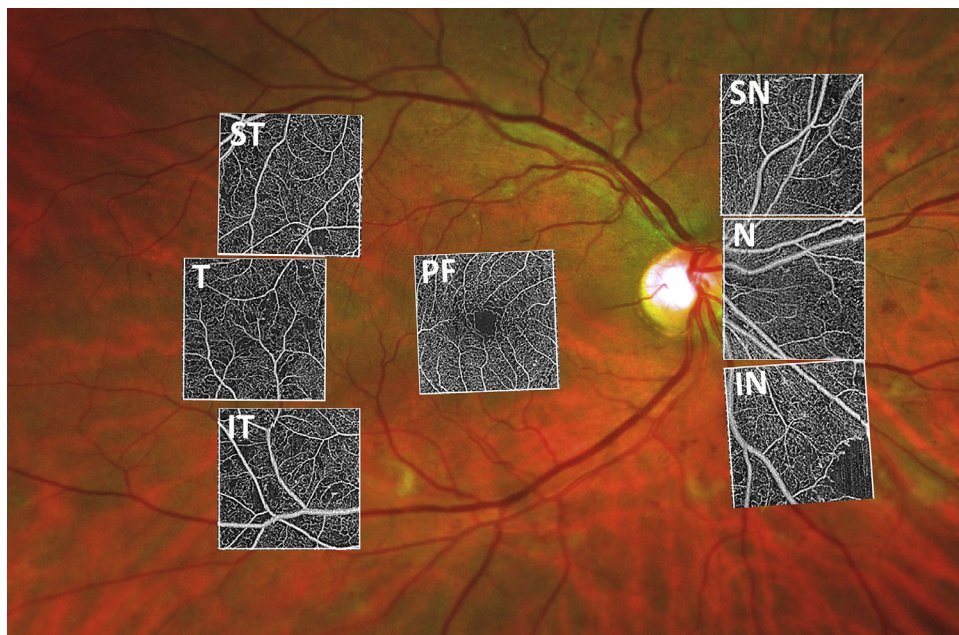


FIGURE 1. The 15 × 15 mm OCTA montage (Plex Elite, Zeiss) of a patient with severe diabetic retinopathy. The position of the seven 3 × 3 mm areas imaged according to our scanning protocol are outlined in the white boxes. PF = parafovea, T = temporal, ST = superior temporal, IT = inferior temporal, N = nasal, SN = superior nasal, IN = inferior nasal.

capillary plexus merge to a single layer approximately 6 to 7 mm temporal to the fovea.¹⁹ Vascular lesions like microaneurysms, dot/blot hemorrhages, and intraretinal microvascular abnormalities are most frequently found temporal to the fovea, and cotton wool spots are predominately seen around the arcades and superonasal or inferonasal to the optic disc.^{20–22} Until now, OCTA images of areas outside the parafovea were either qualitatively analyzed or capillary density measurements were based on wide-field scanning pattern with low resolution, which makes it hard to identify subtle microvascular damage.^{23,24} In the present study, capillary perfusion parameters of 6 predefined 3 × 3 mm areas outside the parafovea (three areas temporal to the fovea and three areas nasal to the optic disc) were compared to the parafovea in patients with different DR severity levels and in healthy control subjects.

METHODS

This prospective, cross-sectional clinical trial was approved by the institutional review board of the University of British Columbia (UBC), Vancouver, British Columbia (BC), Canada (H18-02095), registered at clinicaltrials.gov (NCT03765112), and adhered to the tenants of The Declaration of Helsinki. Patients were recruited at the Department of Ophthalmology and Visual Sciences (UBC, Vancouver, BC, Canada) and written informed consent was obtained. Patients with type 1 or 2 diabetes mellitus (DM), DR of each severity level, and healthy controls were included. The following exclusion criteria were applied: media opacities, active intraocular inflammation, retinal disease other than DR like signs of age-related macular degeneration, drusen, retinal artery or vein occlusion, structural damage to the macula, macular edema with central retinal subfield thickness >290 μm in women and >305 μm in men measured with Spectralis OCT (Heidelberg, Jena, Germany), history of vitrectomy, glaucoma or use of intraocular pressure lowering eye drops, history of

glaucoma surgery, intraocular surgery (including cataract surgery, YAG laser, panretinal laser photocoagulation, intravitreal injection of an anti-VEGF agent or corticosteroids) within 3 months prior to study inclusion. Medical history was obtained, including type of diabetes, duration of diabetes (defined by the start of antidiabetic medication), latest A1c level, height and weight, history of high blood pressure or ongoing anti-hypertensive medication use, history of cardiovascular events (including angina pectoris, myocardial infarction, bypass surgery, STENT implantation, ischemic cardiac disease, and stroke), smoking habits, history of ocular surgery, including lasers, and intravitreal injection therapies.

Image Acquisition

Seven standardized 3 × 3 mm OCTA volumes were recorded with Swept Source Optical Coherence Tomography Angiography (Plex Elite 9000; Carl Zeiss Meditec, Dublin, CA): one was centered on the fovea (C), one superotemporal (ST), one temporal (T) in line with the fovea, and one inferotemporal (IT) each of the latter three at a distance of 15.8° from the fovea by changing the fixation mark nasally to each of the three accustomed fixation options. The other three cubes were recorded nasal to the optic disc: one adjacent to the optic disc (N), one superonasal (SN), and one inferonasal (IN) (Fig. 1). For acquisition of the three nasal areas, the fixation mark was moved temporal to the fovea and the scanning pattern was adjusted next to the optic disc, above, and below. Imaging sequences began with the central 3 × 3 area, followed by the temporal areas, and last, the nasal areas. If both eyes were eligible and the patient was compliant, both eyes were included. For each patient, a 30° macula cube (25 B-scans, high-speed, ART 10) was acquired with Spectralis OCT (Heidelberg Engineering Inc., Heidelberg, Germany) to exclude macular edema and at least one 200° ultra-wide field image was recorded with Optomap (Daytona, Optos Inc.,

Marlborough, MA) for DR severity grading. DR severity grading was done by a retina specialist based on the International Clinical Disease Severity Scale for DR.²⁵

Image Processing

Images with a signal strength greater than eight (out of 10) were included in the study. If the signal strength was eight or lower, the visibility of the capillary networks was evaluated separately to determine if the images could be included in this study. The pseudonymized raw data was exported and analyzed using custom scripts. The inner limiting membrane (ILM), posterior boundary of the inner plexiform layer (IPL), and posterior boundary of the outer plexiform layer (OPL) were then segmented in 3D using an automated graph-cut algorithm implemented in MATLAB.²⁶ Automated segmentations were examined and corrected when necessary by a trained researcher using ITKSnap.²⁷ The OCTA scans were then summed in the axial direction between the segmented layers to produce a projected en face image (Supplementary Fig. S1). The peripapillary plexus and the superficial capillary plexus were summed together from the ILM to posterior boundary of the IPL, and will be referred to as superficial capillary complex (SCC). The intermediate and deep vascular plexuses, which are highly interconnected, were segmented together as the posterior boundary of the IPL to the posterior boundary of the OPL, and will be referred to as DCC.^{19,28,29} The microvasculature was then segmented using a neural network where the output of the network is a grayscale map of the probability that each pixel contains a vessel.³⁰ The maps were then converted to binary by setting every pixel with a probability >50% to 1 and every other pixel to 0. The capillary PD of the SCC and DCC was generated after subtracting the foveal avascular zone (FAZ) area from the capillary pattern in the central scan and the area occupied by blood vessels greater in diameter than capillaries.^{2,31} The FD was also generated for each image using the box-counting method, where the FD is given by $FD = \log(Nr)/\log(r^{-1})$ where Nr is the number of boxes subtended by boxes of ratio r .

Statistics

Sample size calculation was based on the results from Mastropasqua et al., who calculated the parafoveal vessel density of patients with different DR severity levels.³² The results from the superficial capillary plexus were used because they are less susceptible to imaging artifacts compared to the deep capillary plexus. The effect size was the difference in vessel density between mild and moderate/severe DR. A sample size of 23 is needed for a power of 80% and significance level of 5%. Considering a rate of 10% of images unsuitable for further analyses, we included at least 25 patients for each group.

Descriptive statistics were used to summarize and describe patients' characteristics. A Generalized Linear Model (GLM) was fitted to estimate the relationship between different outcomes and patient's characteristics. Given the repeated measure structure of the data and to account for the inter-eye correlation, we used a Generalized Estimating Equation (GEE) method to estimate the GLM parameters for all three outputs (PD/FD of SCC, PD of DCC).³³ In addition, to compare mean of outcomes for different DR severity as well as different areas marginally (unconditional on other patient's characteristics), mean and SD of the three

outcomes were calculated for each of the seven areas separately grouped by DR severity level. To compare the means between severity levels, mean of the three temporal areas were grouped as the temporal group and the mean of the three nasal area was grouped as the nasal group. In the nasal group, for the superficial capillary density and the FD, only the inferior nasal and superior nasal areas were included, because the area right next to the optic disc showed significantly higher values compared with the other two nasal areas. This discrepancy was most probably due to the peripapillary plexus, which was segmented together with the superficial capillary plexus. The Student's *t*-test was used to compare the difference of the three outcomes between patients with DR and healthy control as well as among different DR severity levels. Pearson correlation was computed between diabetes duration and all the three outputs for each DR severity level separately. All analysis was done with R (R version 1.1.447) and with $\alpha = 0.05$ as the significance level (or "familywise" significance level for multiple testing). In the analysis of variance (ANOVA) post hoc multiple comparisons, we reported adjusted *P* values rather than adjusted significance level. Note that in all the comparisons within each area, to overcome the dependency between eyes of the same patient, we used the average of each outcome for a given patient in each area and severity level. In contrast, in the comparisons across different areas, as the effect of area was important to us, we used repeated measure ANOVA to account for the repeated measures of the outcomes of each patient.

RESULTS

One hundred ninety-two eyes (101 OD and 91 OS) of 130 patients were imaged according to the imaging protocol, resulting in 1330 3×3 OCTA volumes in total. Mean signal strength was $9.43 (\pm 0.64)$ and there were only 11 (0.8%) scans with a signal strength lower than 8, which still qualified for further analysis. Scans of patients with mild DR had the best signal strength (mean = 9.65 ± 0.49), whereas patients with moderate/severe DR had the worst signal strength (9.2 ± 0.79 ; $P < 0.001$). The mean signal strength was higher in the center and temporal area (9.6 and 9.49 out of 10, respectively) compared to the three nasal areas (9.31; $P < 0.05$). Patients characteristics are summarized in Table 1.

In general, patients' characteristics were well distributed. There were significantly more female participants in the no-DR group (62%) compared to the moderate/severe group (24%; $P = 0.046$). Diabetes duration and insulin use increased with more severe DR severity levels. Only in the mild DR group the longer diabetes duration was significantly correlated with less PD in the SCC ($r = -0.52$) and DCC ($r = 0.61$) as well as with lower FD ($r = -0.54$). Patients with diabetes had significantly more hypertension ($P < 0.001$) and history of cardiovascular events ($P = 0.016$). All eyes with proliferative DR had a history of panretinal laser treatment ($n = 27$) and/or intravitreal anti-VEGF treatment ($n = 16$). Among the other eyes of patients with diabetes, only three of the moderate/severe group had a history of anti-VEGF treatment and five of the moderate/severe group had a history of focal laser treatment. The results for each outcome grouped by their topographical location for each DR severity level is summarized in Table 2. A pairwise comparison of each location and each DR severity level is illustrated in Supplementary Table S2.

TABLE 1. Patients Characteristics

Variables	Patients Characteristics					
	Control <i>n</i> = 25	No-DR <i>n</i> = 32	Mild <i>n</i> = 27	Mod/sev <i>n</i> = 25	Prolif <i>n</i> = 25	All <i>n</i> = 134
Age, ymean (±SD)	56 (±15)	63 (±16)	61 (±16)	57 (±15)	58 (±12)	59 (±15) <i>P</i> = 0.422
Sex: female (%)	10 (38)	21 (62)	11 (41)	6 (24)	14 (56)	62 (45) <i>P</i> = 0.038 [†]
DM type 1: <i>n</i> (%)	NA	4 (12)	8 (30)	3 (12)	8 (32)	23 (21) [*] <i>P</i> = 0.071
DM duration in years: mean (±SD)	NA	12 (±9)	20 (±14)	17 (±12)	22 (±10)	17 (±12) [*] <i>P</i> = 0.009 [‡]
Insulin use: <i>n</i> (%)	NA	9 (26)	15 (56)	15 (60)	21 (84)	53 (49) [*] <i>P</i> = 0.000 [§]
A1c level	NA	7.3 (±1.3)	7.6 (±1.4)	7.5 (±1.1)	7.8 (±1.5)	7.5 (±1.3) [*] <i>P</i> = 0.730
BMI in kg/m ² :mean (±SD)	26.2 (±3.7)	28.9 (±4.6)	30.2 (±11.1)	27.6 (±3.5)	28.3 (±6.8)	28.3 (±6.6) <i>P</i> = 0.311
Smoking: (yes /used to)	6/3	2/5	3/7	2/5	1/3	14/23 <i>P</i> = 0.390
Hypertension: <i>n</i> (%)	2 (8)	17 (53)	13 (48)	16 (64)	12 (67)	60 (47) <i>P</i> < 0.001
CV event: <i>n</i> (%)	0	5 (15)	6 (22)	8 (32)	7 (28)	26 (19) <i>P</i> = 0.019 [*]
Race: <i>n</i> (%)						<i>P</i> = 0.103
American Indian	0	1 (3)	0	1 (4)	1 (4)	3 (2)
Asian	5 (20)	10 (33)	2 (7)	10 (40)	8 (32)	35 (26)
Black or African American	0	1 (3)	1 (4)	1 (4)	1 (4)	4 (3)
White	18 (72)	16 (50)	21 (78)	12 (48)	12 (48)	79 (59)
More than one race	0	2 (6)	2 (7)	0	1 (4)	5 (4)
Unknown	2 (8)	2 (6)	1 (4)	1 (4)	2 (8)	8 (6)

BMI, body mass index; CV = cardiovascular, NA = not applicable, mod/sev = moderate or severe, prolif = proliferative; five patients had different severity grading in each eye, making the number of patients in this table 134 instead of 129.

^{*} These values are only calculated for patients with diabetes (*n* = 109) excluding healthy controls.

[†] There were significantly more male patients in the moderate/severe group compared to no-DR.

[‡] Patients without DR had significantly shorter duration of diabetes compared to patients with proliferative DR.

[§] Incidence of insulin therapy was significantly less in patients with no-DR compared to patients with moderate/severe and proliferative DR.

^{||} History of hypertension was significantly less prevalent in controls compared to patients with diabetes of any severity level.

^{*} There were significantly less CV events in controls compared to patients with moderate/severe DR.

Significance levels between groups were calculated with analysis of variance (ANOVA) for scale variables and chi-square test for nominal variables.

TABLE 2. Summary of Quantitative OCTA Features for Different DR Severity Levels

Outcomes	Area	Healthy Control <i>n</i> = 33	No-DR <i>n</i> = 51	Mild <i>n</i> = 41	Mod/Severe	Proliferative
		Mean (± SD)	Mean (± SD)	Mean (± SD)	<i>n</i> = 37 Mean (± SD)	<i>n</i> = 30 Mean (± SD)
PD of SCC	Parafovea	0.50 (0.02)	0.50 (0.02)	0.48 (0.03)	0.45 (0.04)	0.42 (0.04)
	Temporal	0.46 (0.02) [*]	0.47 (0.03) [*]	0.45 (0.04) [*]	0.39 (0.05)[*]	0.33 (0.07)[*]
	Nasal	0.45 (0.04) [*]	0.46 (0.03) [*]	0.46 (0.04) [*]	0.40 (0.05)[*]	0.35 (0.08)[*]
FD of SCC	Parafovea	1.72 (0.01)	1.72 (0.01)	1.71 (0.01)	1.70 (0.01)	1.68 (0.02)
	Temporal	1.70 (0.01) [*]	1.71 (0.01) [*]	1.70 (0.01) [*]	1.68 (0.02)[*]	1.65 (0.05)[*]
	Nasal	1.71 (0.01) [*]	1.70 (0.01) [*]	1.70 (0.01) [*]	1.68 (0.02)[*]	1.66 (0.05)[*]
PD of DCC	Parafovea	0.49 (0.02)	0.48 (0.03)	0.47 (0.02)	0.44 (0.04)	0.43 (0.05)
	Temporal	0.50 (0.02)	0.48 (0.02)	0.48 (0.03)	0.41 (0.07)	0.39 (0.09)
	Nasal	0.50 (0.03)	0.48 (0.03)	0.47 (0.03)	0.38 (0.08)	0.39 (0.08)

Outcomes grouped according to retinal topography of 3 × 3 mm scanning areas. For the outcomes of the SCC, the area directly nasal to the optic disc was excluded because it showed significantly higher values than the supero- and inferonasal areas. Values in bold letters are significantly different to outcomes of DR severity one stage lower. Values marked with * are significantly different to values measured in the parafovea. The *P* values were adjusted according to the Tukey multiple testing method.

Mod = moderate.

Topography of Perfusion Density

There was no significant difference between sex for any of the four outcomes at any severity level. The SCC showed a significantly higher mean capillary density (*P* < 0.001) in the central 3 × 3 volume, compared to five of the six other locations measured at all DR severity levels as well as in healthy controls (Supplementary Table S3). Only in the area nasal to the optic disc were the perfusion densities of the SCC and the FD both comparable to the fovea. Hence, measures of the SCC (mean PD and mean FD) were summarized for the three temporal areas but only measures of the supero- and inferonasal areas were summarized for the nasal areas

in Table 2 and Figure 2. In contrast, the DCC showed similar PD across all areas measured (Supplementary Table S3).

Comparison of Perfusion Density Between Different DR Severity Levels

The DCC showed a significant difference of capillary PD between no-DR and control only in the temporal and nasal areas, respectively (*P* < 0.001). When looking at each of the seven areas separately, significant changes were seen at the areas of the nasal inferior (*P* = 0.009) and just temporal to the fovea (*P* = 0.022) between no-DR and control. The PD of

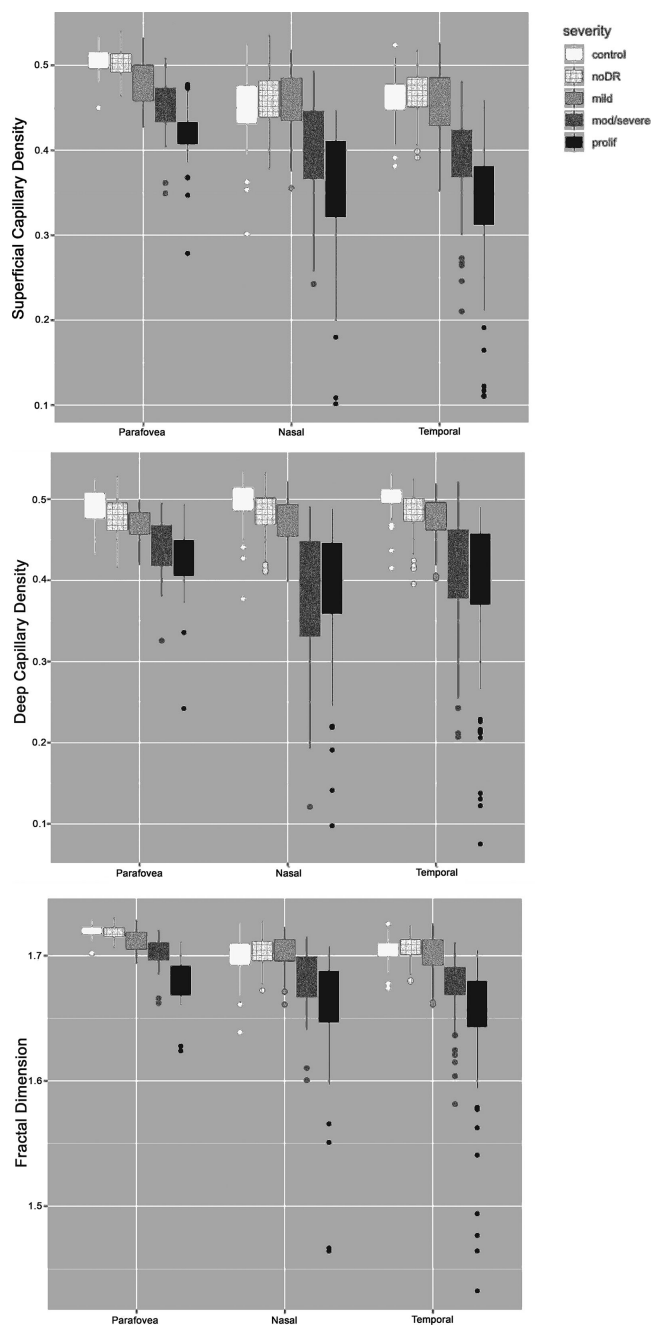


FIGURE 2. Plot of the three main outcomes (perfusion density of the superficial and deep capillary plexus as well as fractal dimension of the superficial capillary plexus) for each severity level of diabetic retinopathy grouped by retinal topography of the scanning pattern. The nasal and temporal areas show overall higher variability in each outcome compared to the center. Similarly, the difference between mild and moderate/severe diabetic retinopathy is best visible in the nasal/temporal areas. The bottom and top of each box are the 25th (Q_1) and 75th (Q_3) percentile, respectively. The upper and lower whiskers are $Q_1 - 1.5$ interquartile range (IQR) and $Q_3 + 1.5$ IQR, respectively.

the DCC further dropped with increasing DR severity, showing significant difference in all areas between mild and no-DR as well as between moderate/severe and mild DR. Mean PD in proliferative DR was the least of all severity levels.

In the SCC, the PD and FD were comparable between no-DR eyes and controls (Table 2). However, PD and FD in

the SCC were significantly less in the central 3×3 scan in patients with mild DR compared to controls ($P < 0.001$), whereas PD and FD in the SCC were significantly less in the central and temporal areas in mild compared to no-DR. PD of the SCC further dropped with increasing DR severity showing significant differences in all areas between moderate/severe and mild DR as well as between proliferative and moderate/severe DR.

DISCUSSION

In this study, perfusion parameters of patients of each DR severity level and healthy controls were evaluated in 7 defined 3×3 mm areas scanned with high resolution swept-source OCTA. Perfusion density of the DCC was significantly reduced ($P < 0.001$) outside the parafovea in patients without DR compared to controls, whereas no difference was seen in the parafovea (Table 2). The DCC was also primarily affected in patients with type 1 DM without DR.³⁴ In these patients, a rarefaction of the DCC was also described in the parafovea, whereas the area temporal to the fovea was not evaluated. Capillary loss in the temporal macula coincides with the topographic preference of microaneurysm formation.^{21,35–37} Early blood flow impediment in the DCC might lead to endothelial cell and pericyte loss, and consequently to microaneurysm formation, which are most frequently located in the inner nuclear layer of the retina.^{38–40} It is known that peripheral areas reveal better risk stratification of DR disease progression than the parafovea.⁴¹ Half of the patients with severe capillary loss in the more peripheral areas progress to proliferative diabetic retinopathy (PDR) within a year. Looking for capillary loss outside the central macula, especially in the nasal and temporal areas, can reveal advanced disease, which is not apparent from the area around the fovea only.

Although the PD of the DCC were already less in early disease, there was a temporary trend toward higher PD in the SCC in patients without DR compared to controls (Table 2, Figure 2) before PD also started to decrease in the SCC in more severe disease. Similar results were published by Rosen et al., who also excluded noncapillary blood vessel from the PD analysis.⁴² Recently, Palochak et al. described an increased blood flow velocity in vessels of the SCC measured with Adaptive optics scanning laser ophthalmoscopy (AOSLO) in early diabetes.⁴³ The selective measurement of relatively small blood vessels (15–100 μm in diameter) of the SCC allows new and detailed insight into retinal hemodynamics. Increased retinal perfusion before the occurrence of retinal lesions secondary to DR was described previously.^{44,45} Again, this trend was more pronounced in the nasal and temporal areas. Redirected blood flow from the DCC to the SCC might enhance the perfusion of the SCC and result in higher blood flow velocity. Blood flow through otherwise unperfused capillaries, which were found to be prevalent in healthy young adults by Pinhas et al. could explain the higher PD measurements of the SCC in our patients without DR.⁴⁶ Our results in patients with diabetes without DR are likely to be based on functional instead of structural factors influencing retinal hemodynamics. With increasing DR severity (moderate/severe and proliferative DR), PD of the SCC significantly decreases in all areas measured.

In healthy controls, a topographic variation in PD of the SCC in the parafoveal area is previously described.^{47,48} Although wide-field OCTA covers a larger area, accurate

PD measurements are limited by the sampling density.^{23,49} Compared to larger scanning patterns, 3×3 mm scans were found to be the best for predicting the presence or absence of DR.²³ We chose to acquire 3×3 mm volumes with the highest sampling density available at different areas of the macula by changing the fixation target to predefined settings. With this approach we achieve the best resolution currently possible for Swept Source OCTA imaging. The mean PD of the SCC was greatest in the central 3×3 mm area, which parallels the higher ganglion cell/inner plexiform layer thickness around the fovea.⁵⁰ Our results of topographical differences in PD are consistent with Campbell et al.¹⁹ Five of the six peripheral areas showed a similar PD of the SCC, which was decreasing with increasing DR severity. Only the area nasal to the optic nerve head showed a significantly greater PD ($P < 0.05$) compared to the other peripheral areas. The higher PD nasal to the optic nerve head can be attributed to a thicker radial peripapillary plexus closer to the optic nerve head, which was segmented together with the superficial capillary plexus. Due to their proximity within the retina, the peripapillary and the superficial plexuses were not segmented individually, although a separation of both is possible in a research setting.⁵¹ In contrast, the PD of the DCC was similar in all areas measured, which is consistent with a uniform inner nuclear layer (INL)/IPL thickness of the macula. Again, the intermediate and deep vascular plexuses were not segmented separately due to their proximity and high connectivity.²⁸

All three outcomes showed a higher variability of perfusion parameters with increasing DR severity in the nasal and temporal locations compared to the central location. The higher variability in PD measures reveals that different severities of capillary loss can be present with a similar amount of clinically visible lesions. In fact, the PD of the DCC in proliferative DR was not significantly different from moderate/severe DR, so extensive capillary dropout in the DCC occurs relatively early in the disease. Capillary PD measured outside the parafovea could serve as a new biomarker and might add to the risk stratification of DR progression in patients with diabetes.

However, there are certain limitations to OCTA imaging. Acquiring scans from seven designated areas can be time consuming. Although acquisition time was not measured in this study, overall signal strength was worse in the nasal areas, which came last in the imaging sequence. Further studies are needed to evaluate if image quality is dependent on the scanning location or the sequence of acquisition. It might be sufficient to reduce the image acquisition to one scan temporal and/or one nasal of the macula (SN and IN) to reflect the overall perfusion status of these areas, because the PD within five of the peripheral areas (ST, T, IT, SN, and IN) was similar ($P > 0.05$) in the SCC and DCC. Scanning the area temporal to the fovea (T) might be the easiest in terms of image post processing. This area is usually void of bigger vessels, which need to be subtracted before the capillary PD can be calculated accurately. According to our results, the PD of the DCC at the area just temporal to the fovea was significantly less in no-DR compared to control. In addition, in the clinic, the temporal region of the parafovea is the most sensitive to predict the onset of DR.³²

Nasally and temporally, the scanned areas might vary slightly interindividually depending on the patient's head position or ocular rotation, however, the distance to the fovea remains consistent. All outcomes were calculated as mean of the 3×3 mm area so slight deviations of the scan-

ning position might not impact the results. Last, the intermediate and deep vascular plexuses were combined as DCC and not evaluated separately. Although these two capillary networks can be evaluated separately in the parafovea, they converge further temporally to a single plexus.

To conclude, OCTA technology allows for an objective and quantitative analysis of capillary perfusion of different retina areas in patients with diabetes and different DR severity levels. A decrease in PD in the DCC outside the parafovea was an early sign of disease in patients without clinical signs of DR.

Acknowledgments

The authors thank the support by the Diabetes Action Canada (a CIHR SPOR group) for this work.

Disclosure: **S.G. Karst**, None; **M. Heisler**, None; **J. Lo**, None; **N. Schuck**, None; **A. Safari**, None; **M.V. Sarunic**, Seymour Vision Inc. (I); **D.A.L. Maberley**, None; **E.V. Navajas**, None

References

- International Diabetes Federation. *Eighth Edition 2017*. 2017. doi: [http://dx.doi.org/10.1016/S0140-6736\(16\)31679-8](http://dx.doi.org/10.1016/S0140-6736(16)31679-8).
- Kim AY, Chu Z, Shahidzadeh A, Wang RK, Puliafito CA, Kashani AH. Quantifying microvascular density and morphology in diabetic retinopathy using spectral-domain optical coherence tomography angiography. *Invest Ophthalmol Vis Sci*. 2016;57:OCT362–OCT370.
- Simonett JM, Scarinci F, Picconi F, et al. Early microvascular retinal changes in optical coherence tomography angiography in patients with type 1 diabetes mellitus. *Acta Ophthalmol*. 2017;95:e751–e755.
- Dimitrova G, Chihara E, Takahashi H, Amano H, Okazaki K. Quantitative retinal optical coherence tomography angiography in patients with diabetes without diabetic retinopathy. *Investig Ophthalmology Vis Sci*. 2017;58:190.
- Vujosevic S, Toma C, Villani E, et al. Early detection of microvascular changes in patients with diabetes mellitus without and with diabetic retinopathy: comparison between different swept-source OCT-A instruments. 2019;2019:2547216.
- Soares M, Neves C, Marques IP, et al. Comparison of diabetic retinopathy classification using fluorescein angiography and optical coherence tomography angiography. *Br J Ophthalmol*. 2017;101:62–68.
- Chen Q, Ma Q, Wu C, et al. Macular vascular fractal dimension in the deep capillary layer as an early indicator of microvascular loss for retinopathy in type 2 diabetic patients. *Investig Ophthalmol Vis Sci*. 2017;58:3785–3794.
- Tang FY, Ng DS, Lam A, et al. Determinants of quantitative optical coherence tomography angiography metrics in patients with diabetes. *Sci Rep*. 2017;7:1–10.
- Scarinci F, Picconi F, Giorno P, et al. Deep capillary plexus impairment in patients with type 1 diabetes mellitus with no signs of diabetic retinopathy revealed using optical coherence tomography angiography. *Acta Ophthalmol*. 2018;96:e264–e265.
- Agemy SA, Scripsema NK, Shah CM, et al. Retinal vascular perfusion density mapping using optical coherence tomography angiography in normals and diabetic retinopathy patients. *Retina*. 2015;35:2353–2363.
- Nesper PL, Roberts PK, Onishi AC, et al. Quantifying microvascular abnormalities with increasing severity of diabetic retinopathy using optical coherence tomography

- angiography. *Invest Ophthalmol Vis Sci.* 2017;58:307–315.
12. Lee J, Rosen R. Optical coherence tomography angiography in diabetes. *Curr Diab Rep.* 2016;16:123.
 13. Czakó C, Sándor G, Ecsedy M, et al. Decreased retinal capillary density is associated with a higher risk of diabetic retinopathy in patients with diabetes. *Retina.* 2019;39:1710–1719.
 14. Akil H, Karst S, Heisler M, Etmnan M, Navajas E, Maberley D. Application of optical coherence tomography angiography in diabetic retinopathy: a comprehensive review. *Can J Ophthalmol.* 2019;54:519–528.
 15. Cao D, Yang D, Huang Z, et al. Optical coherence tomography angiography discerns preclinical diabetic retinopathy in eyes of patients with type 2 diabetes without clinical diabetic retinopathy. *Acta Diabetol.* 2018;55:469–477.
 16. Zahid S, Dolz-Marco R, Freund KB, et al. Fractal dimensional analysis of optical coherence tomography angiography in eyes with diabetic retinopathy. *Investig Ophthalmol Vis Sci.* 2016;57:4940–4947.
 17. Silva PS, Cavallerano JD, Haddad NMN, et al. Peripheral lesions identified on ultrawide field imaging predict increased risk of diabetic retinopathy progression over 4 years. *Ophthalmology.* 2015;122:949–956.
 18. Silva PS, El-Rami H, Barham R, et al. Hemorrhage and/or microaneurysm severity and count in ultrawide field images and early treatment diabetic retinopathy study photography. *Ophthalmology.* 2016;124:970–976.
 19. Campbell JP, Zhang M, Hwang TS, et al. Detailed vascular anatomy of the human retina by projection-resolved optical coherence tomography angiography. *Sci Rep.* 2017;7:42201.
 20. Sears CM, Nittala MG, Jayadev C, et al. Comparison of subjective assessment and precise quantitative assessment of lesion distribution in diabetic retinopathy. *JAMA Ophthalmol.* 2018;136:365–371.
 21. Dobree JH. Simple diabetic retinopathy. Evolution of the lesions and therapeutic considerations. *Br J Ophthalmol.* 1970;54:1–10.
 22. Howard-Williams JR, Peckar CO, Holman RR, Turner RC, Bron AJ. Quantifying early diabetic retinopathy. *Diabetologia.* 1986;29:761–766.
 23. Hirano T, Kitahara J, Toriyama Y, Kasamatsu H, Murata T, Sadda S. Quantifying vascular density and morphology using different swept-source optical coherence tomography angiographic scan patterns in diabetic retinopathy. *Br J Ophthalmol.* 2019;103:216–221.
 24. Mastropasqua R, D'Aloisio R, Di Antonio L, et al. Wide-field optical coherence tomography angiography in diabetic retinopathy. *Acta Diabetol.* 2019;56:1293–1303.
 25. Wilkinson CP, Ferris FL, Klein RE, et al. Proposed international clinical diabetic retinopathy and diabetic macular edema disease severity scales. *Ophthalmology.* 2003;110:1677–1682.
 26. Lee S, Fallah N, Forooghian F, et al. Comparative analysis of repeatability of manual and automated choroidal thickness measurements in nonneovascular age-related macular degeneration. *Invest Ophthalmol Vis Sci.* 2013;54:2864–2871.
 27. Yushkevich PA, Piven J, Hazlett HC, et al. User-guided 3D active contour segmentation of anatomical structures: significantly improved efficiency and reliability. *Neuroimage.* 2006;31:1116–1128.
 28. Leahy C, Radhakrishnan H, Weiner G, Goldberg JL, Srinivasan VJ. Mapping the 3D connectivity of the rat inner retinal vascular network using OCT angiography. *Investig Ophthalmol Vis Sci.* 2015;56:5785–5793.
 29. Onishi AC, Nesper PL, Roberts PK, et al. Importance of considering the middle capillary plexus on OCT angiography in diabetic retinopathy. *Investig Ophthalmol Vis Sci.* 2018;59:2167–2176.
 30. Prentas P, Heisler M, Mammo Z, et al. Segmentation of the foveal microvasculature using deep learning networks. *J Biomed Opt.* 2016;21:75008.
 31. Scripsema NK, Garcia PM, Bavier RD, et al. Optical coherence tomography angiography analysis of perfused peripapillary capillaries in primary open-angle glaucoma and normal-tension glaucoma. *Invest Ophthalmol Vis Sci.* 2016;57:OCT611–OCT620.
 32. Mastropasqua R, Toto L, Mastropasqua A, et al. Foveal avascular zone area and parafoveal vessel density measurements in different stages of diabetic retinopathy by optical coherence tomography angiography. *Int J Ophthalmol.* 2017;10:1545–1551.
 33. Ying G, Maguire MG, Glynn R, Rosner B. Tutorial on biostatistics: statistical analysis for correlated binary eye data. *Ophthalmic Epidemiol.* 2018;25:1–12.
 34. Carnevali A, Sacconi R, Corbelli E, et al. Optical coherence tomography angiography analysis of retinal vascular plexuses and choriocapillaris in patients with type 1 diabetes without diabetic retinopathy. *Acta Diabetol.* 2017;54:695–702.
 35. Bek T, Helgesen A. The regional distribution of diabetic retinopathy lesions may reflect risk factors for progression of the disease. *Acta Ophthalmol Scand.* 2001;79:501–505.
 36. Tang J, Mohr S, Du Y-D, Kern TS. Non-uniform distribution of lesions and biochemical abnormalities within the retina of diabetic humans. *Curr Eye Res.* 2003;27:7–13.
 37. Kern TS, Engerman RL. Vascular lesions in diabetes are distributed non-uniformly within the retina. *Exp Eye Res.* 1995;60:545–549.
 38. Horii T, Murakami T, Nishijima K, Sakamoto A, Ota M, Yoshimura N. Optical coherence tomographic characteristics of microaneurysms in diabetic retinopathy. *Am J Ophthalmol.* 2010;150:840–848.
 39. Moore J, Bagley S, Ireland G, McLeod D, Boulton ME. Three dimensional analysis of microaneurysms in the human diabetic retina. *J Anat.* 1999;194:89–100.
 40. Stitt AW, Gardiner TA, Archer DB. Histological and ultrastructural investigation of retinal microaneurysm development in diabetic patients. *Br J Ophthalmol.* 1995;79:362–367.
 41. ETDRS Research Group. Fluorescein angiographic risk factors for progression of diabetic retinopathy. ETDRS report number 13. Early Treatment Diabetic Retinopathy Study Research Group. *Ophthalmology.* 1991;98(5 Suppl.):834–840.
 42. Rosen RB, Andrade Romo JS, Krawitz BD, et al. Earliest evidence of preclinical diabetic retinopathy revealed using optical coherence tomography angiography perfused capillary density. *Am J Ophthalmol.* 2019;203:103–115.
 43. Palochak CMA, Lee HE, Song J, et al. Retinal blood velocity and flow in early diabetes and diabetic retinopathy using adaptive optics scanning laser ophthalmoscopy. *J Clin Med.* 2019;8:E1165.
 44. Pemp B, Schmetterer L. Ocular blood flow in diabetes and age-related macular degeneration. *Can J Ophthalmol.* 2008;43:295–301.
 45. Grunwald JE, DuPont J, Riva CE. Retinal haemodynamics in patients with early diabetes mellitus. *Br J Ophthalmol.* 1996;80:327–331.
 46. Pinhas A, Razeen M, Dubow M, et al. Assessment of perfused foveal microvascular density and identification of nonperfused capillaries in healthy and vasculopathic eyes. *Invest Ophthalmol Vis Sci.* 2014;55:8056–8066.
 47. Krawitz BD, Phillips E, Bavier RD, et al. Parafoveal nonperfusion analysis in diabetic retinopathy using optical

- coherence tomography angiography. *Transl Vis Sci Technol.* 2018;7:4.
48. Sleightholm MA, Arnold J, Kohner EM. Diabetic retinopathy: I. The measurement of intercapillary area in normal retinal angiograms. *J Diabet Complications.* 1988;2:113–116.
 49. Agemy SA, Scripsema NK, Shah CM, et al. Retinal vascular perfusion density mapping using optical coherence tomography angiography in normals and diabetic retinopathy patients. *Retina.* 2015;35:2353–2363.
 50. Hassan M, Sadiq MA, Halim MS, et al. Evaluation of macular and peripapillary vessel flow density in eyes with no known pathology using optical coherence tomography angiography. *Int J Retin Vitr.* 2017;3:27.
 51. Park JJ, Soetikno BT, Fawzi AA. Characterization of the middle capillary plexus using optical coherence tomography angiography in healthy and diabetic eyes. *Retina.* 2016;36:2039–2050.